

Peridynamic Damage Model Based on Absolute Bond Elongation

Shangyuan Zhang and Yufeng Nie[✉]

Research Center for Computational Science, Northwestern Polytechnical University,
Xi'an 710129, P.R. China
zhangshangyuan@mail.nwpu.edu.cn, yfnie@nwpu.edu.cn

Abstract. A bond-based peridynamic damage model is proposed to incorporate the deformation and the damage process into a unified framework. This new model is established based on absolute bond elongation, and both the elastic and damage parameters of the material are embedded in the constitutive relationship, which makes the model better characterize the process of material damage. Finally, different phenomenons for various damage patterns is observed by numerical experiments, rich damage patterns will make this model better suitable for damage simulation.

Keywords: Damage · Peridynamic · Bond-based · Absolute bond elongation.

1 Introduction

Peridynamic [19] provides an alternative theory to classical continuum mechanics in modeling complex crack problems. Different from the classical continuum mechanics, the mechanical behavior of the material is characterized by nonlocal interactions between material points. The spatial derivative of the displacement in the model is replaced by the integration. It is this feature makes it an advantage in dealing with crack propagation problems. Its effectiveness in modeling material damage has been shown in numerical simulation of crack nucleation [21], crack propagation [15] and branching [13,4], phase transformations in solids [6], impact damage [3] and so on. Mathematical analysis and numerical approximation of the peridynamic model have been studied in [8,11,9,10,5].

Silling and Askari introduced a peridynamic damage model in [20]. However, in this model, the damage is a function of the bond stretch (the rate of elongation), which is not continuous about bond stretch. This brings a lot of trouble to the well-posedness of the model in mathematics. It is impossible to describe the process of the bond from elastic deformation to damage and finally failure. Yang et. al. [7] proposed a damage model to investigate mode-I crack propagation in concrete by constructing a trilinear softening curve of the bond stretch. For the first time, Emmrich give a well-posed result for a nonlinear peridynamic model with Lipschitz continuous pairwise force function [9], and extended it to inherit irreversible damage [10]. To make the model accurately describe the fracture

phenomenon, there are two main problems need to be considered. One is how to involve damage in the constitutive relationship of the material. The other is the mechanism of crack nucleation in fracture. The absolute bond elongation contains higher order deformation than the stretch, it can describe deformation better. It is essential for the peridynamic model to integrate these components into the model.

Based on the above viewpoints, a peridynamic damage model is established based on absolute bond elongation, and the fracture criterion based on absolute bond elongation is also given. By setting the damage term to be continuous, the well-posedness could be ensured. The ability to treat both the deformation and damage within the same mathematical framework will make the peridynamic model a practical tool to simulate the whole process of the real material deformation.

This paper is organized as follows. The peridynamic damage model for PMB (Prototype Microelastic Brittle) material is presented in Section 2. Then, the damage model based on bond elongation are presented in Section 3. Finally, numerical experiments are then presented in Section 4, showing that the effects of different damage patterns on material fracture behavior and further discussing the peridynamic modeling.

2 The peridynamic theory

The equation of motion for the bond-based peridynamic model is

$$\rho \ddot{\mathbf{u}}(\mathbf{x}, t) = \int_{\mathcal{H}_x} \mathbf{f}(\mathbf{u}(\mathbf{x}', t) - \mathbf{u}(\mathbf{x}, t), \mathbf{x}' - \mathbf{x}) dV_{\mathbf{x}'} + \mathbf{b}(\mathbf{x}, t), \quad (x, t) \in \Omega \times (0, T). \quad (1)$$

where ρ denotes the mass density, \mathcal{H}_x is the peridynamic neighborhood of $\mathbf{x} \in \Omega$, \mathbf{f} is the pairwise force function, \mathbf{b} is the external force density, the vector $\boldsymbol{\xi} = \mathbf{x}' - \mathbf{x}$ denotes the relative position vector between the two material points, which we call bond. $\boldsymbol{\eta} = \mathbf{u}(\mathbf{x}', t) - \mathbf{u}(\mathbf{x}, t)$ represents the relative displacement. The interaction between the material points will decrease with the distance increasing, once the distance between the two material points beyond the horizon δ , the interaction $\mathbf{f}(\boldsymbol{\eta}, \boldsymbol{\xi}) = \mathbf{0}$ ($|\boldsymbol{\xi}| > \delta$). The bond stretch is the relative change of the bond, which is defined as follows

$$s(\boldsymbol{\xi}, \boldsymbol{\eta}) = \frac{|\boldsymbol{\eta} + \boldsymbol{\xi}| - |\boldsymbol{\xi}|}{|\boldsymbol{\xi}|}. \quad (2)$$

For PMB material, the pairwise force function is proportional to the bond stretch. In order to describe the damage phenomenon, a damage indicator is multiplied in original constitutive relation [20], and the constitutive relation can be written as

$$\mathbf{f}(\boldsymbol{\eta}, \boldsymbol{\xi}) = cs(\boldsymbol{\xi}, \boldsymbol{\eta})\mu(\boldsymbol{\xi}, \boldsymbol{\eta}) \frac{\boldsymbol{\eta} + \boldsymbol{\xi}}{|\boldsymbol{\eta} + \boldsymbol{\xi}|}, \quad (3)$$

Then the spring constant c can be expressed with the known material constants in the classical theory [2]. $\mu(\boldsymbol{\xi}, \boldsymbol{\eta})$ is the bond damage indicator, and its expression is

$$\mu(\boldsymbol{\xi}, \boldsymbol{\eta}) = \begin{cases} 1, & \text{otherwise} \\ 0, & \exists t' \in [0, t], \text{ s.t. } s(\boldsymbol{\xi}, \boldsymbol{\eta}(t')) > s_0. \end{cases} \quad (4)$$

Here, s_0 is critical bond stretch that might be determined from experimental data. However, since there exists a jump break point at the critical stretch, which brings the difficulty in the proof of the well-posedness.

3 The peridynamic with damage

In our model, both the elastic and damage parameters of the material are embedded in the constitutive relationship. Besides, the absolute bond elongation contains more deformation information than the bond stretch. The damage model based on absolute bond elongation is given as follows

$$\mathbf{f}(\boldsymbol{\eta}, \boldsymbol{\xi}) = \omega(|\boldsymbol{\xi}|)e(|\boldsymbol{\eta} + \boldsymbol{\xi}|, |\boldsymbol{\xi}|)\mu(\boldsymbol{\xi}, e)\frac{\boldsymbol{\eta} + \boldsymbol{\xi}}{|\boldsymbol{\eta} + \boldsymbol{\xi}|}. \quad (5)$$

The ω is the influence function, which reflects that the different bond have effect on its own force and the material property, $e = |\boldsymbol{\eta} + \boldsymbol{\xi}| - |\boldsymbol{\xi}|$ is the absolute bond elongation. Two common forms of influence function in the literature [20,4] are given as follows.

(a) PMB material: $\omega(|\boldsymbol{\xi}|) = \frac{c}{|\boldsymbol{\xi}|}$. (b) Soda-Lime Glass: $\omega(|\boldsymbol{\xi}|) = \frac{c}{|\boldsymbol{\xi}|} \left(1 - \frac{|\boldsymbol{\xi}|}{\delta}\right)$. In constitutive relation (5), μ is a function of absolute bond elongation e , and its forms were constructed by using Hermite interpolation, such as

(i) The function itself is continuous:

$$\mu(e) = \begin{cases} 1, & \text{if } e < \lambda e_c(|\boldsymbol{\xi}|), \\ \frac{e_c - e}{e_c - \lambda e_c}, & \text{if } \lambda e_c(|\boldsymbol{\xi}|) \leq e \leq e_c(|\boldsymbol{\xi}|), \\ 0, & \text{if } e > e_c(|\boldsymbol{\xi}|). \end{cases} \quad (6)$$

(ii) First-order derivative function is continuous:

$$\mu(e) = \begin{cases} 1, & \text{if } e < \lambda e_c(|\boldsymbol{\xi}|), \\ 1 - \frac{3(e - \lambda e_c)^2}{(e_c - \lambda e_c)^2} + \frac{2(e - \lambda e_c)^3}{(e_c - \lambda e_c)^3}, & \text{if } \lambda e_c(|\boldsymbol{\xi}|) \leq e \leq e_c(|\boldsymbol{\xi}|), \\ 0, & \text{if } e > e_c(|\boldsymbol{\xi}|). \end{cases} \quad (7)$$

(iii) Second-order derivative function is continuous:

$$\mu(e) = \begin{cases} 1, & \text{if } e < \lambda e_c(|\boldsymbol{\xi}|), \\ 1 - \frac{10(e - \lambda e_c)^3}{(e_c - \lambda e_c)^3} + \frac{15(e - \lambda e_c)^4}{(e_c - \lambda e_c)^4} - \frac{6(e - \lambda e_c)^5}{(e_c - \lambda e_c)^5}, & \text{if } \lambda e_c(|\boldsymbol{\xi}|) \leq e \leq e_c(|\boldsymbol{\xi}|), \\ 0, & \text{if } e > e_c(|\boldsymbol{\xi}|). \end{cases} \quad (8)$$

Where λ is the parameter given in the computing process, and $e_c(|\xi|)$ is the critical elongation of each bond. If we assume that $\omega(|\xi|)$ has form (a) or (b), and $e_c(|\xi|) = d|\xi|^s$, then the peridynamic damage model based on absolute bond elongation is obtained. We now turn to determine the model parameters. It should be noticed that the determination of c is before the damage ($\mu = 1$).

3.1 Determination of elastic constants

Influence function in form (a) Assumed that $\omega(|\xi|) = \frac{c}{|\xi|}$ and the body undergo a homogeneous deformation, that is $\eta = \epsilon\xi$, then the bond elongation $e = \epsilon|\xi|$. Therefore, the energy in bond ξ is

$$W_{bond} = \int_0^{\epsilon|\xi|} \frac{c}{|\xi|} e \, de = \frac{c\epsilon^2|\xi|}{2}. \quad (9)$$

The energy density at x is

$$W_{nonlocal} = \frac{1}{2} \int_{\mathcal{H}_x} W_{bond} dV x' = \begin{cases} \int_0^\delta \frac{c\epsilon^2\xi}{4} 4\pi\xi^2 d\xi = \frac{\pi c\epsilon^2\delta^4}{4}, & D = 3, \\ h_2 \int_0^\delta \frac{c\epsilon^2\xi}{4} 2\pi\xi d\xi = \frac{\pi c h_2 \epsilon^2 \delta^3}{6}, & D = 2, \\ h_1 \int_0^\delta \frac{c\epsilon^2\xi}{4} 2d\xi = \frac{c h_1 \epsilon^2 \delta^2}{4}, & D = 1. \end{cases} \quad (10)$$

Undergo the same deformation, the strain energy density of the classical theory is

$$W_{classical}^{3D} = \frac{9k\epsilon^2}{2}, \quad W_{classical}^{2D} = 2k'\epsilon^2, \quad W_{classical}^{1D} = \frac{E\epsilon^2}{2}. \quad (11)$$

then we obtain that

$$c^{3D} = \frac{18k}{\pi\delta^4}, \quad c^{2D} = \frac{12k'}{\pi h_2 \delta^3}, \quad c^{1D} = \frac{2E}{h_1 \delta^2}. \quad (12)$$

where k and k' is the bulk modulus in 3D and 2D respectively, E is the Young's modulus, h_1 and h_2 is the rod cross-sectional area and plate thickness.

Influence function in form (b) Assumed that $\omega(|\xi|) = \frac{c}{|\xi|} \left(1 - \frac{|\xi|}{\delta}\right)$, then the energy in bond ξ is

$$W_{bond} = \int_0^{\epsilon|\xi|} \frac{c}{|\xi|} \left(1 - \frac{|\xi|}{\delta}\right) e \, de = \frac{c\epsilon^2|\xi|}{2} \left(1 - \frac{|\xi|}{\delta}\right) \quad (13)$$

The energy density at x is

$$W_{nonlocal} = \frac{1}{2} \int_{\mathcal{H}_x} W_{bond} dV_{x'} = \begin{cases} \int_0^\delta \frac{c\epsilon^2 |\xi|}{4} \left(1 - \frac{|\xi|}{\delta}\right) 4\pi \xi^2 d\xi = \frac{\pi c \epsilon^2 \delta^4}{20}, & D = 3, \\ h_2 \int_0^\delta \frac{c\epsilon^2 |\xi|}{4} \left(1 - \frac{|\xi|}{\delta}\right) 2\pi \xi d\xi = \frac{\pi c h_2 \epsilon^2 \delta^3}{24}, & D = 2, \\ h_1 \int_0^\delta \frac{c\epsilon^2 |\xi|}{4} \left(1 - \frac{|\xi|}{\delta}\right) 2d\xi = \frac{c h_1 \epsilon^2 \delta^2}{12}, & D = 1. \end{cases} \quad (14)$$

Undergo the same deformation, the strain energy density of the classical theory is

$$W_{classical}^{3D} = \frac{9k\epsilon^2}{2}, \quad W_{classical}^{2D} = 2k'\epsilon^2, \quad W_{classical}^{1D} = \frac{E\epsilon^2}{2}, \quad (15)$$

then we obtain that

$$c^{3D} = \frac{90k}{\pi\delta^4}, \quad c^{2D} = \frac{48k'}{\pi h_2 \delta^3}, \quad c^{1D} = \frac{6E}{h_1 \delta^2}. \quad (16)$$

where k and k' is the bulk modulus in 3D and 2D respectively, E is the Young's modulus, h_1 and h_2 is the rod cross-sectional area and plate thickness.

3.2 Determination of damage constants

If we assume that $e_c(|\xi|) = d|\xi|^s$, then we need to determine the parameter d for bond damage. Assume the bond undergo a elongation such that the bond broken, The superscripts below are used to represent the energy under different influence functions and damage patterns. Using following formulation

$$W_{bondbroken} = \int_0^{e_c} \omega(|\xi|) e \mu(e) de. \quad (17)$$

Then the energy in a single bond under different patterns can be written as

- $W_{bondbroken}^{ai} = \frac{cd^2 |\xi|^{2s-1} (\lambda^2 + \lambda + 1)}{6},$
- $W_{bondbroken}^{aai} = \frac{cd^2 |\xi|^{2s-1} (3\lambda^2 + 4\lambda + 3)}{20},$
- $W_{bondbroken}^{aaii} = \frac{cd^2 |\xi|^{2s-1} (2\lambda^2 + 3\lambda + 2)}{14},$
- $W_{bondbroken}^{bi} = cd^2 |\xi|^{2s-1} \left(1 - \frac{|\xi|}{\delta}\right) \frac{\lambda^2 + \lambda + 1}{6},$
- $W_{bondbroken}^{bii} = cd^2 |\xi|^{2s-1} \left(1 - \frac{|\xi|}{\delta}\right) \frac{3\lambda^2 + 4\lambda + 3}{20},$
- $W_{bondbroken}^{biii} = cd^2 |\xi|^{2s-1} \left(1 - \frac{|\xi|}{\delta}\right) \frac{2\lambda^2 + 3\lambda + 2}{14}.$

Next, we will obtain the parameters in one, two and three dimensions.

3D Case The critical energy release rate in 3D case can be expressed as

$$G_0 = \int_0^\delta \int_0^{2\pi} \int_z^\delta \int_0^{\cos^{-1}z/\xi} W_{bondbroken} \xi^2 \sin\phi d\phi d\xi d\theta dz. \quad (18)$$

Then the damage constant in different influence function and damage patterns will be calculated as

$$\begin{aligned} d^{ai} &= \sqrt{\frac{6(2s+3)G_0}{\pi c \delta^{2s+3}(1+\lambda+\lambda^2)}}, & d^{bi} &= \sqrt{\frac{6(2s+3)(2s+4)G_0}{\pi c \delta^{2s+3}(1+\lambda+\lambda^2)}}, \\ d^{aii} &= \sqrt{\frac{20(2s+3)G_0}{\pi c \delta^{2s+3}(3+4\lambda+3\lambda^2)}}, & d^{bii} &= \sqrt{\frac{20(2s+3)(2s+4)G_0}{\pi c \delta^{2s+3}(3+4\lambda+3\lambda^2)}}, \\ d^{aiii} &= \sqrt{\frac{14(2s+3)G_0}{\pi c \delta^{2s+3}(2+3\lambda+2\lambda^2)}}, & d^{biii} &= \sqrt{\frac{14(2s+3)(2s+4)G_0}{\pi c \delta^{2s+3}(2+3\lambda+2\lambda^2)}}. \end{aligned} \quad (19)$$

2D Case The critical energy release rate in 2D case can be expressed as

$$G_0 = 2h \int_0^\delta \int_z^\delta \int_0^{\cos^{-1}z/\xi} W_{bondbroken} \xi d\phi d\xi dz. \quad (20)$$

Then the damage constant in different influence function and damage patterns in 2D case will be obtained as follows.

$$\begin{aligned} d^{ai} &= \sqrt{\frac{6G_0}{chF_a(1+\lambda+\lambda^2)}}, & d^{bi} &= \sqrt{\frac{6G_0}{chF_b(1+\lambda+\lambda^2)}}, \\ d^{aii} &= \sqrt{\frac{20G_0}{chF_a(3+4\lambda+3\lambda^2)}}, & d^{bii} &= \sqrt{\frac{20G_0}{chF_b(3+4\lambda+3\lambda^2)}}, \\ d^{aiii} &= \sqrt{\frac{14G_0}{chF_a(2+3\lambda+2\lambda^2)}}, & d^{biii} &= \sqrt{\frac{14G_0}{chF_b(2+3\lambda+2\lambda^2)}}, \end{aligned} \quad (21)$$

where

$$F_a = \frac{\delta^{2+2s} \left(4s + \frac{1}{1+s} + \frac{\sqrt{\pi}\Gamma(-1-s)}{\Gamma(-1/2-s)} \right) + \frac{2\delta^{2+2s}\sqrt{\pi}\Gamma(-s)}{(2+2s)\Gamma(-1/2-s)}}{(1+2s)^2}, \quad (22)$$

$$F_b = \frac{\delta^{2+2s}}{3+5s+2s^2}, \quad (23)$$

are the functions used in (21), h is the thickness of the plate. However, there is *Gamma* function in (22), which is not exist in some case, we can use three-dimensional damage parameters as an alternative way.

1D Case The critical energy release rate in 1D case can be expressed as

$$G_0 = h \int_0^\delta \int_z^\delta W_{bondbroken} d\xi dz. \quad (24)$$

Then the damage constant in different influence function and damage patterns in 1D case can be calculated as

$$\begin{aligned} d^{ai} &= \sqrt{\frac{6(2s+1)G_0}{ch\delta^{2s+1}(1+\lambda+\lambda^2)}}, & d^{bi} &= \sqrt{\frac{6(2s+2)(2s+1)G_0}{ch\delta^{2s+1}(1+\lambda+\lambda^2)}}, \\ d^{aai} &= \sqrt{\frac{20(2s+1)G_0}{ch\delta^{2s+1}(3+4\lambda+3\lambda^2)}}, & d^{bii} &= \sqrt{\frac{20(2s+2)(2s+1)G_0}{ch\delta^{2s+1}(3+4\lambda+3\lambda^2)}}, \\ d^{aaii} &= \sqrt{\frac{14(2s+1)G_0}{ch\delta^{2s+1}(2+3\lambda+2\lambda^2)}}, & d^{biii} &= \sqrt{\frac{14(2s+2)(2s+1)G_0}{ch\delta^{2s+1}(2+3\lambda+2\lambda^2)}}, \end{aligned} \quad (25)$$

where h is the cross sectional area of the bar.

3.3 Conservation of Energy and Energy Decay

The peridynamic damage model based on absolute bond elongation is given as follows:

$$\begin{cases} \rho \ddot{\mathbf{u}}(t, \mathbf{x}) = \int_{\Omega \cup \Omega_c} \omega(|\mathbf{x}' - \mathbf{x}|) f(e(t, \mathbf{x}, \mathbf{x}', \mathbf{u})) \mu(e, e^*) \mathbf{M}(t, \mathbf{x}, \mathbf{x}', \mathbf{u}) d\mathbf{x}' \\ \quad + \mathbf{b}(t, \mathbf{x}), \\ \mathbf{u}(0, \mathbf{x}) = \mathbf{w}(\mathbf{x}), \quad \dot{\mathbf{u}}(0, \mathbf{x}) = \mathbf{v}(\mathbf{x}), \quad \mathbf{u}(t, \cdot)|_{\Omega_c} = 0. \end{cases} \quad (26)$$

where ρ is the mass density, the term $\omega_\delta(\mathbf{x}' - \mathbf{x})$ is the influence function, $f(e(t, \mathbf{x}, \mathbf{x}', \mathbf{u})) = ce(t, \mathbf{x}, \mathbf{x}', \mathbf{u})$ reflects the relationship between the magnitude of the bond force and the bond elongation, e is bond elongation, e^* is the largest bond elongation in historical time, $\mu(e, e^*)$ denotes the damage, $\mathbf{M}(t, \mathbf{x}, \mathbf{x}', \mathbf{u})$ indicates the direction of the bond force, $\mathbf{b}(t, \mathbf{x})$ is the body force. Assume that external forces don't change over time, the total energy of the system is

$$\begin{aligned} E(t) &= \frac{1}{2} \int_{\Omega \cup \Omega_c} \int_{\Omega \cup \Omega_c} \omega(|\mathbf{x}' - \mathbf{x}|) p(e(t, \mathbf{x}, \mathbf{x}', \mathbf{u})) d\mathbf{x}' d\mathbf{x} \\ &\quad + \frac{1}{2} \int_{\Omega} \rho |\dot{\mathbf{u}}(t, \mathbf{x})|^2 d\mathbf{x} - \int_{\Omega} \mathbf{u}(t, \mathbf{x}) \cdot \mathbf{b}(\mathbf{x}) d\mathbf{x}. \end{aligned} \quad (27)$$

where $\omega_\delta(|\mathbf{x}' - \mathbf{x}|) p(e)$ is the energy produced by the deformation of a single bond.

$$p(e) = \int_0^e f(e') \mu(e', e^*) de' \quad (28)$$

Theorem 1. (*Conservation of Energy and Energy Decay*) *If the bond never broken, the total energy of system (26) is conserved. If the bond broken, the total energy of system (26) is nonincreasing in time.*

Proof.

$$\begin{aligned}
\frac{dE(t)}{dt} &= \int_{\Omega} \rho \dot{\mathbf{u}}(t, \mathbf{x}) \cdot \ddot{\mathbf{u}}(t, \mathbf{x}) d\mathbf{x} - \int_{\Omega} \dot{\mathbf{u}}(t, \mathbf{x}) \cdot \mathbf{b}(\mathbf{x}) d\mathbf{x} \\
&+ \frac{1}{2} \int_{\Omega \cup \Omega_{\mathcal{I}}} \int_{\Omega \cup \Omega_{\mathcal{I}}} \omega_{\delta}(|\mathbf{x}' - \mathbf{x}|) f(e) \mu(e, e^*) \dot{e}(t, \mathbf{x}, \mathbf{x}', \mathbf{u}) d\mathbf{x}' d\mathbf{x} \\
&+ \frac{1}{2} \int_{\Omega \cup \Omega_{\mathcal{I}}} \int_{\Omega \cup \Omega_{\mathcal{I}}} \omega_{\delta}(|\mathbf{x}' - \mathbf{x}|) \left(\int_0^e f(e') \frac{d\mu(e, e^*)}{de^*} de' \right) \dot{e}^*(t, \mathbf{x}, \mathbf{x}', \mathbf{u}) d\mathbf{x}' d\mathbf{x} \\
&= \int_{\Omega} \rho \dot{\mathbf{u}}(t, \mathbf{x}) \cdot \ddot{\mathbf{u}}(t, \mathbf{x}) d\mathbf{x} - \int_{\Omega} \dot{\mathbf{u}}(t, \mathbf{x}) \cdot \mathbf{b}(\mathbf{x}) d\mathbf{x} \\
&+ \frac{1}{2} \int_{\Omega \cup \Omega_{\mathcal{I}}} \int_{\Omega \cup \Omega_{\mathcal{I}}} \omega_{\delta}(|\mathbf{x}' - \mathbf{x}|) f(e) \mu(e) \mathbf{M}(t, \mathbf{x}, \mathbf{x}', \mathbf{u}) (\dot{\mathbf{u}}(t, x') - \dot{\mathbf{u}}(t, x)) d\mathbf{x}' d\mathbf{x} \\
&+ \frac{1}{2} \int_{\Omega \cup \Omega_{\mathcal{I}}} \int_{\Omega \cup \Omega_{\mathcal{I}}} \omega_{\delta}(|\mathbf{x}' - \mathbf{x}|) \left(\int_0^e f(e') \frac{d\mu(e, e^*)}{de^*} de' \right) \dot{e}^*(t, \mathbf{x}, \mathbf{x}', \mathbf{u}) d\mathbf{x}' d\mathbf{x} \\
&= \int_{\Omega} \rho \dot{\mathbf{u}}(t, \mathbf{x}) \cdot \ddot{\mathbf{u}}(t, \mathbf{x}) d\mathbf{x} - \int_{\Omega} \dot{\mathbf{u}}(t, \mathbf{x}) \cdot \mathbf{b}(\mathbf{x}) d\mathbf{x} \\
&- \int_{\Omega \cup \Omega_{\mathcal{I}}} \int_{\Omega \cup \Omega_{\mathcal{I}}} \omega_{\delta}(|\mathbf{x}' - \mathbf{x}|) f(e) \mu(e) \mathbf{M}(t, \mathbf{x}, \mathbf{x}', \mathbf{u}) \dot{\mathbf{u}}(t, x) d\mathbf{x}' d\mathbf{x} \\
&+ \frac{1}{2} \int_{\Omega \cup \Omega_{\mathcal{I}}} \int_{\Omega \cup \Omega_{\mathcal{I}}} \omega_{\delta}(|\mathbf{x}' - \mathbf{x}|) \left(\int_0^e f(e') \frac{d\mu(e, e^*)}{de^*} de' \right) \dot{e}^*(t, \mathbf{x}, \mathbf{x}', \mathbf{u}) d\mathbf{x}' d\mathbf{x} \\
&= \frac{1}{2} \int_{\Omega \cup \Omega_{\mathcal{I}}} \int_{\Omega \cup \Omega_{\mathcal{I}}} \omega_{\delta}(|\mathbf{x}' - \mathbf{x}|) \left(\int_0^e f(e') \frac{d\mu(e, e^*)}{de^*} de' \right) \dot{e}^*(t, \mathbf{x}, \mathbf{x}', \mathbf{u}) d\mathbf{x}' d\mathbf{x}.
\end{aligned}$$

In the above process, we need the integrand is continuous. If bond never broken, then $\dot{e}^*(t, \mathbf{x}, \mathbf{x}', \mathbf{u}) = 0$, and $\frac{dE(t)}{dt} = 0$, the total energy of system (26) is conserved. When bond broking, because the damage is a nonincreasing function and the bond can't recover, $\frac{d\mu}{de^*} \leq 0$, then $\frac{dE(t)}{dt} \leq 0$, the total energy of the system is decreasing. So when bondbroken happening, the system will have the energy decay property, that is said the system consistent with the laws of thermodynamics.

4 Numerical examples

In this section, numerical examples are given to demonstrate the effectiveness of the model, and the meshfree method [16] is used to solve the model equation. First, the body is discretized into material points, and the equation have the form

$$\rho \ddot{\mathbf{u}}_i = \sum_{p \in \mathcal{H}_{\delta}(x_i)} \mathbf{f}(\mathbf{u}_p - \mathbf{u}_i, \mathbf{x}_p - \mathbf{x}_i) V_p + b_i, i = 1, 2, \dots, N. \quad (29)$$

Then, the equation in the time direction can be discretized as follows.

$$\rho \left(\frac{\mathbf{u}_i^{n+1} - 2\mathbf{u}_i^n + \mathbf{u}_i^{n-1}}{\Delta t^2} \right) = \sum_p \mathbf{f}(\mathbf{u}_p^n - \mathbf{u}_i^n, \mathbf{x}_p - \mathbf{x}_i) V_p + b_i^n, i = 1, 2, \dots, N. \quad (30)$$

that is,

$$\rho \left(\frac{\dot{\mathbf{u}}_i^{n+1} - \dot{\mathbf{u}}_i^n}{\Delta t} \right) = \sum_p \mathbf{f}(\mathbf{u}_p^n - \mathbf{u}_i^n, \mathbf{x}_p - \mathbf{x}_i) V_p + b_i^n, i = 1, 2, \dots, N. \quad (31)$$

Where

$$\dot{\mathbf{u}}_i^{n+1} = \frac{\mathbf{u}_i^{n+1} - \mathbf{u}_i^n}{\Delta t}. \quad (32)$$

Therefore, rewriting the above procedure in the following format.

$$\mathbf{u}_i^{n+1} = \dot{\mathbf{u}}_i^{n+1} \Delta t + \mathbf{u}_i^n, i = 1, 2, \dots, N. \quad (33)$$

$$\dot{\mathbf{u}}_i^{n+1} = \ddot{\mathbf{u}}_i^{n+1} \Delta t + \dot{\mathbf{u}}_i^n, i = 1, 2, \dots, N. \quad (34)$$

In following numerical experiments, numerical results under different damage relations are given, and the damage areas are highlighted to show the impact of different damage on numerical simulation. The damage index ϕ whose definition is given by

$$\phi(\mathbf{x}, t) = 1 - \frac{\int_{B_\delta(\mathbf{x})} \mu dV_{x'}}{\int_{B_\delta(\mathbf{x})} dV_{x'}}, \quad (35)$$

where μ is the bond damage factor.

4.1 Example 1

A simple benchmark problem in dynamic fracture is performed using the peridynamic damage model based on bond elongation to investigate the influence of different influence functions and continuity on numerical results. A thin square plate with a pre-existing crack which subjected to a velocity boundary condition is given below. To verify the validity of the model and the influence of different damage models. Numerical simulation results in several modes are presented. The geometry of the plate can be seen in figure 1, the thickness of the plate is 0.1 mm, pre-existing crack length is 10 mm at the center. In the process of

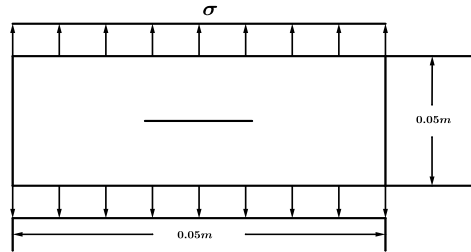


Fig. 1. Geometry of the plate with pre-existing crack in the center

Table 1. Material parameters for the plate

ρ	$E(\text{Gpa})$	ν	$G_0(\text{J/m}^2)$
2450	32	1/3	3.0

computing, grid spacing is 0.1 mm. The mechanical properties of the material is presented in Table 1. Where E is Young modulus, ν is the Poisson ratio, ρ is density, and G_0 is the critical energy release rate. The uniform normal stress is applied to the top and bottom edges of the plate perpendicular to the crack. The figure is the result at $20.05\mu\text{s}$, similar experiments can be seen in [1,18].

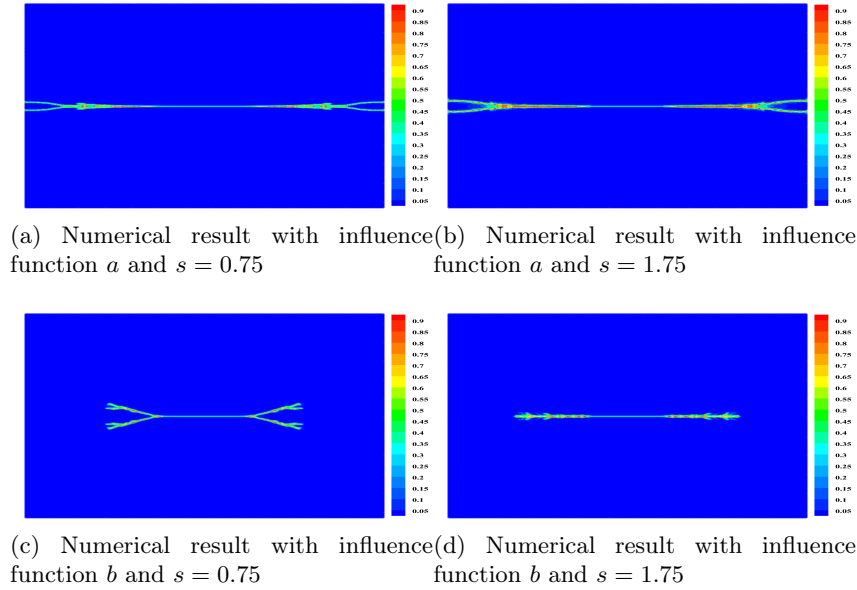
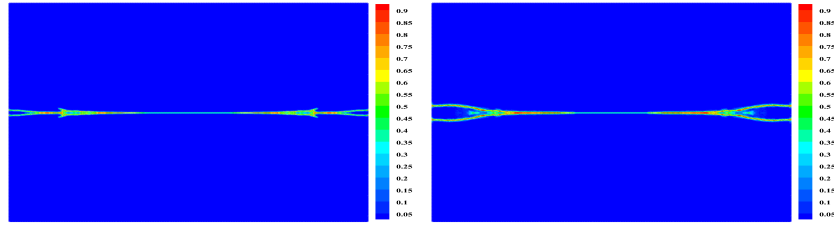
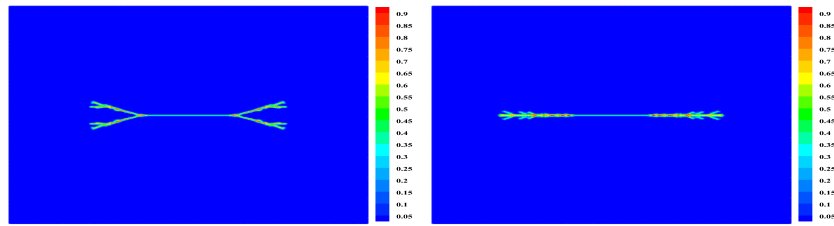
**Fig. 2.** damage is continuous about the bond elongation

Figure 2, 3, 4 show the damage contour plots in the plate when the damage is zero, first and second-order continuous about the bond elongation, respectively. This may reveal some differences that might arise due to the continuity of the damage. It is observed from the plots that as the continuity of the damage increasing, there was little change in the damage contour plots. It can be understood that increasing the continuity doesn't change the energy in a single bond breaking a lot. But this might preserve some underlying physical properties.

In figure 2, 3, 4, the subfigure a and b are the result for influence function (a) with stress 5 Mpa, the subfigure c and d are the results for influence function (b) with stress 5 Mpa. It should be noticed that when the influence function changed, the energy in a single bond changed a lot, different crack propagation

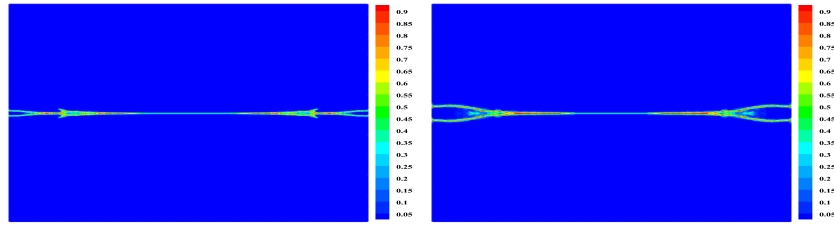


(a) Numerical result with influence function a and $s = 0.75$ (b) Numerical result with influence function a and $s = 1.75$

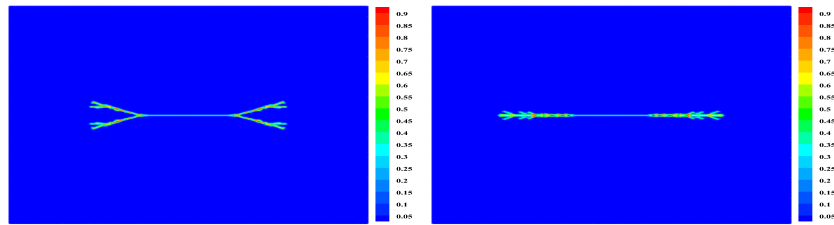


(c) Numerical result with influence function b and $s = 0.75$ (d) Numerical result with influence function b and $s = 1.75$

Fig. 3. damage is first order continuous about the bond elongation



(a) Numerical result with influence function a and $s = 0.75$ (b) Numerical result with influence function a and $s = 1.75$



(c) Numerical result with influence function b and $s = 0.75$ (d) Numerical result with influence function b and $s = 1.75$

Fig. 4. damage is second order continuous about the bond elongation

phenomenon can be observed. When s changed, the energy of bond-breaking is also changed, so different damage patterns were observed. It is an advantage that for different physical materials, the real description of physical phenomena can be achieved by adjusting parameters.

4.2 Example 2

A simple benchmark problem in dynamic fracture is performed using the peridynamic damage model based on bond elongation to investigate the effectiveness of our model. The dynamic crack propagation and branching can be observed in the numerical simulation. The problem considered here is that of crack branching in a plate made of glass subjected to sudden stress loading conditions. This problem has been simulated with peridynamic damage model [12,14,17], and the experiment result can also be seen in [13]. As shown in figure 5, the setup consists of a plate with a pre-crack from the left edge to the center of the plate. The material properties considered are in table 2, and the influence function a

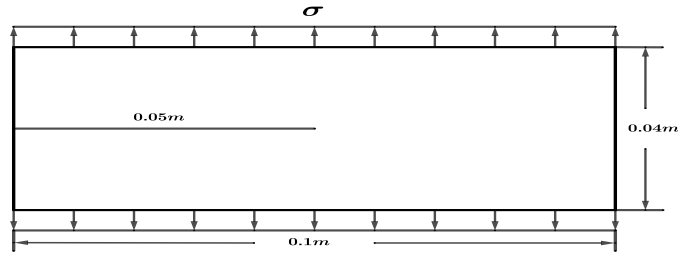


Fig. 5. Configuration of the plate

is used in the experiment. The plate is loaded dynamically at the top and bottom surfaces with a sustained stress of 1.2 Mpa . A regular lattice of material particles is used for the discretization, the lattice spacing of 0.1 mm is used, the horizon chosen is three times the lattice spacing. Figure 6a shows the damage

Table 2. Material parameters for the plate

ρ	$E(\text{Gpa})$	ν	$G_0(\text{J/m}^2)$
2440	72	1/3	3.8

contour in the plate at 1.2 Mpa . It becomes very clear from this figure that the crack branching happened. The peridynamic damage model predicts symmetrical crack path with simple branching. As it can be seen in figure 6a, this result coincides with the experiments [13] reported by Ha and Bobaru in Fig.

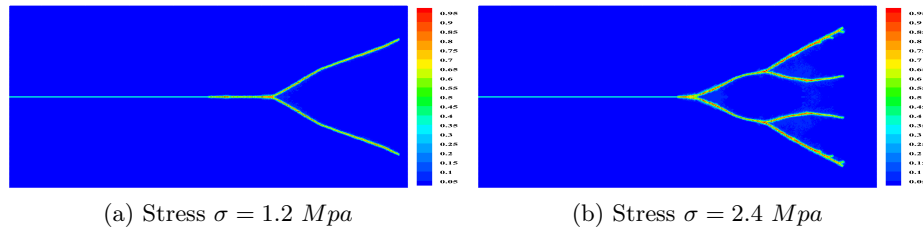


Fig. 6. Crack propagation in the plate with stress $\sigma = 1.2 \text{ Mpa}$, 2.4 Mpa

8. With increasing the applied force, the number of crack branch is increasing. Figure 6b presents the results while the applied load is increased up to 2.4 Mpa . As observed from the damage plots in figure 6b, a secondary crack branching is observed by peridynamic model. This result confirms by experiments [13] in Fig. 8.

5 Conclusions

A new peridynamic damage model is proposed which is based on absolute bond elongation. In this model, the elastic parameters and damage parameters are embedded into the constitutive relation, so that the whole process of the material from elastic to the damage can be modeled. Moreover, the effects of different influence functions and different damage patterns are investigated numerically. In particular, a pre-cracked plate under applied traction is simulated to assess the accuracy of the model and the numerical results agree better with the crack branching experiment. However, the mechanism of fracture and damage is very complex, the parameter in this model is depending on the classical model, it is not accurate for describing the fracture problem. In the future, extending the model based on experimental and molecular dynamics will enable the model to effectively describe the practical problem.

Acknowledgements This research was supported by National Natural Science Foundation of China(No.11971386) and the National Key R&D Program of China(No. 2020YFA0713603).

References

1. Abbasiniyan, L., Hoseini, S.h., faroughi, S.: Fracture analysis of pre-cracked and notched thin plates using peridynamic theory. Journal of Computational and Applied Research in Mechanical Engineering (2019). <https://doi.org/10.22061/jcarme.2019.5136.1628>
2. Bobaru, F., Foster, J.T., Geubelle, P.H., Silling, S.A.: Handbook of peridynamic modeling. CRC press (2016)

3. Bobaru, F., Ha, Y.D., Hu, W.: Damage progression from impact in layered glass modeled with peridynamics. *Central European Journal of Engineering* **2**(4), 551–561 (2012)
4. Bobaru, F., Zhang, G.: Why do cracks branch? a peridynamic investigation of dynamic brittle fracture. *International Journal of Fracture* **196**(1-2), 59–98 (2015)
5. Chen, X., Gunzburger, M.: Continuous and discontinuous finite element methods for a peridynamics model of mechanics. *Computer Methods in Applied Mechanics and Engineering* **200**(9-12), 1237–1250 (2011)
6. Dayal, K., Bhattacharya, K.: Kinetics of phase transformations in the peridynamic formulation of continuum mechanics. *Journal of the Mechanics and Physics of Solids* **54**(9), 1811–1842 (2006)
7. Dong, Y., Wei, D., Xuefeng, L., Shenghui, Y., Xiaoqiao, H.: Investigation on mode-I crack propagation in concrete using bond-based peridynamics with a new damage model. *Engineering Fracture Mechanics* **199**, 567 – 581 (2018)
8. Du, Q., Tao, Y., Tian, X.: A peridynamic model of fracture mechanics with bond-breaking. *Journal of Elasticity* **132**(2), 197–218 (Aug 2018)
9. Emmrich, E., Puhst, D.: Well-posedness of the peridynamic model with lipschitz continuous pairwise force function. *Communications in Mathematical Sciences* **11**(4), 1039–1049 (2013)
10. Emmrich, E., Puhst, D.: A short note on modeling damage in peridynamics. *Journal of Elasticity* **123**(2), 245–252 (Apr 2016)
11. Emmrich, E., Weckner, O.: The peridynamic equation and its spatial discretisation. *Mathematical Modelling and Analysis* **12**(1), 17–27 (2007)
12. Ha, Y.D., Bobaru, F.: Studies of dynamic crack propagation and crack branching with peridynamics. *International Journal of Fracture* **162**(1-2), 229–244 (2010)
13. Ha, Y.D., Bobaru, F.: Characteristics of dynamic brittle fracture captured with peridynamics. *Engineering Fracture Mechanics* **78**(6), 1156–1168 (2011)
14. Huang, D., Lu, G., Wang, C., Qiao, P.: An extended peridynamic approach for deformation and fracture analysis. *Engineering Fracture Mechanics* **141**, 196–211 (2015)
15. Kilic, B., Madenci, E.: Prediction of crack paths in a quenched glass plate by using peridynamic theory. *International Journal of Fracture* **156**(2), 165–177 (2009)
16. Madenci, E., Oterkus, E.: *Peridynamic Theory and Its Applications*. Springer New York, New York, NY (2014)
17. Prakash, N., Seidel, G.D.: A novel two-parameter linear elastic constitutive model for bond based peridynamics. In: *56th AIAA/ASCE/AHS/ASC Structures, Structural Dynamics, and Materials Conference* (2015)
18. Ramulu, M., Kobayashi, A.S.: Mechanics of crack curving and branching — a dynamic fracture analysis. *International Journal of Fracture* **27**(C5), 187–201 (1985)
19. Silling, S.: Reformulation of elasticity theory for discontinuities and long-range forces. *Journal of the Mechanics and Physics of Solids* **48**(1), 175–209 (2000)
20. Silling, S.A., Askari, E.: A meshfree method based on the peridynamic model of solid mechanics. *Computers & structures* **83**(17-18), 1526–1535 (2005)
21. Silling, S.A., Weckner, O., Askari, E., Bobaru, F.: Crack nucleation in a peridynamic solid. *International Journal of Fracture* **162**(1-2), 219–227 (2010)